Chapter 3

Hosotani's approach to the Schwinger model

In the 1990s, Yukio Hosotani *et al.* published several studies of the massive Schwinger model for an arbitrary number of flavors N at finite temperature T, where they reduced the massive model to a quantum mechanical system of $N-1$ degrees of freedom. This allowed them to derive analytic predictions for the boson masses that appear in the model and for the chiral condensate as well. In the massless N flavor model, it is known that a boson of mass $\mu = \sqrt{Ng^2/\pi}$ appears. On the other hand, in the Schwinger model with degenerate non-zero fermion mass the approach by Hosotani gives as a result N bosons, $N-1$ of them with the same mass μ_2 and one with mass $\mu_1 > \mu_2$. If $m \to 0$ then $\mu_2 \to 0$ and $\mu_1 \to \mu$ [1, 2].

We will revise the most important equations of this appproach without the derivation of them, together with a numerical solution that gives predictions of the boson masses and the chiral condensate for the two flavor model at finite temperature. Unfortunately, the reliability of these solutions is limited to $m \ll \mu$.

3.1 Reduction to a quantum mechanical system

The QED Lagrangian for the N flavor Schwinger model is given by

$$\mathcal{L} = -\frac{1}{4}F_{\mu\nu}F^{\mu\nu} + \sum_{f=1}^{N}\overline{\psi}_f\left[\gamma^\mu\left(i\partial_\mu - gA_\mu\right) - m_f\right]\psi_f. \tag{3.1}$$

The index f denotes the flavor. We are going to consider degenerate fermion masses, that is $m_f \equiv m$.

The first step is to map the Schwinger model onto a circle of circumference L_t and to impose the following boundary conditions of the fermion fields and the gauge field

$$\begin{aligned} \psi_f(t, x+L_t) &= -e^{2\pi i\alpha_f}\psi_f(t,x), \\ A_\mu(t, x+L_t) &= e^{2\pi i\alpha_f}A_\mu(t,x), \end{aligned} \tag{3.2}$$

where α_f is a phase factor. It is important to note that if one performs a Wick rotation $it \to x$ and then interchanges $x \leftrightarrow \tau$, with τ the Euclidean time, then the boundary condition is

$$\begin{aligned} \psi_f\left(\tau + \frac{1}{T}, x\right) &= -e^{2\pi i\alpha_f}\psi_f(\tau,x), \\ A_\mu\left(\tau + \frac{1}{T}, x\right) &= e^{2\pi i\alpha_f}A_\mu\left(\tau,x\right), \end{aligned} \tag{3.3}$$

where $T = \frac{1}{L_t}$ is the temperature (see ref. [3]). That way, by setting $\alpha_f = 0$ it is possible to relate the model on the circle with the finite temperature one, which is of interest.

Next one uses the *bosonization method* to reduce the model to a quantum mechanical system of $N-1$ degrees of freedom. The main idea is to write the fields in terms of bosonic operators that obey certain commutation relations, see e.g. refs. [2, 4]. However, those steps are rather tedious and here we only review the resulting formulation. After bosonization, the following equation

$$\hat{H}\,|\Phi_0\rangle = E_0\,|\Phi_0\rangle\,, \tag{3.4}$$

where $|\Phi_0\rangle$ is the vacuum state and E_0 its energy, is reduced to

$$\begin{aligned}
&[-\triangle_\varphi + \kappa F_N(\varphi_1,...,\varphi_N)]\, g(\varphi_1,...,\varphi_N) = \epsilon g(\varphi_1,...,\varphi_N),\\
&\kappa_0 = \frac{N}{\pi(N-1)} m L_t \overline{B} e^{-\pi/\mu N L_t},\quad F_N(\varphi_1,...,\varphi_N) = -\sum_{f=1}^{N}\cos\varphi_f,\\
&\overline{B} = [B(\mu_1 L_t)]^{1/N}\,[B(\mu_2 L_t)]^{1-(1/N)},\quad \epsilon = \frac{N L_t E_0}{2\pi} + \frac{\pi N^2}{12},\\
&B(z) = \frac{z}{4\pi}\exp\left[\gamma + \frac{\pi}{z} - 2\int_1^\infty \frac{du}{(e^{uz}-1)\sqrt{u^2-1}}\right].
\end{aligned} \tag{3.5}$$

$\gamma = 0.57721566490...$ is the Euler-Mascheroni constant, ϵ has to be determined together with $g(\varphi_1,...,\varphi_N)$ and φ_f are angular variables constrained by

$$\varphi_N = \theta - \sum_{f=1}^{N-1}\varphi_f. \tag{3.6}$$

θ is the vacuum angle, it can be restricted to $(-\pi,\pi)$. $\triangle_\varphi$ is the Laplacian of the system, given by

$$\begin{aligned}
\triangle_\varphi &= \sum_{f=1}^{N-1}\left(\frac{\partial}{\varphi_f} - i\beta_f\right)^2 - \frac{2}{N-1}\sum_{f<f'}^{N-1}\left(\frac{\partial}{\partial\varphi_f} - i\beta_f\right)\left(\frac{\partial}{\partial\varphi_{f'}} - i\beta_{f'}\right)\\
&\beta_f = \alpha_f - \alpha_N.
\end{aligned} \tag{3.7}$$

The first line in eq. (3.5) is an eigenvalue problem for a system of $N-1$ degrees of freedom, due to the restriction (3.6). These equations enable us to find solutions for μ_2 (see below). First we simplify eqs. (3.5) for $N = 2$. The Laplacian is now given by

$$\triangle_\varphi = \left(\frac{d}{d\varphi_1} + i\delta\alpha\right)^2 = \frac{1}{i^2}\left(i\frac{d}{d\varphi} - \delta\alpha\right)^2 = -\left(i\frac{d}{d\varphi} - \delta\alpha\right)^2, \tag{3.8}$$

with $\delta\alpha = \alpha_2 - \alpha_1$. On the other hand, in virtue of the constriction (3.6), the function $F_2(\varphi_1,\varphi_2)$ can be written as

$$F_2(\varphi_1) = -\cos(\varphi_1) - \cos(\varphi_1 - \theta). \tag{3.9}$$

It is possible to rewrite the last expression as $-2\cos\frac{\theta}{2}\cos\left(\varphi_1 - \frac{\theta}{2}\right)$, this can be seen using

trigonometric identities

$$\begin{aligned} -2\cos\frac{\theta}{2}\cos\left(\varphi_1-\frac{\theta}{2}\right) &= -2\cos^2\frac{\theta}{2}\cos\varphi_1+2\cos\frac{\theta}{2}\sin\frac{\theta}{2}\sin\varphi_1 \\ &= -2\left(\frac{1+\cos\theta}{2}\right)\cos\varphi_1+\sin\theta\sin\varphi_1 \\ &= -\cos\varphi_1-\cos\theta\cos\varphi_1+\sin\theta\sin\varphi_1 \\ &= -\cos\varphi_1-\cos(\varphi_1-\theta). \end{aligned} \tag{3.10}$$

Substituting the result for $\triangle_\varphi$ and $F_2(\varphi_1)$ in eq. (3.5) yields

$$\left[\left(i\frac{d}{d\varphi_1}-\delta\alpha\right)^2-2\kappa_0\cos\frac{\theta}{2}\cos\left(\varphi_1-\frac{\theta}{2}\right)\right]g(\varphi_1)=\epsilon g(\varphi_1). \tag{3.11}$$

Let us define

$$\kappa\equiv 2\kappa_0\cos\frac{\theta}{2}=\frac{4}{\pi}mL_t\cos\frac{\theta}{2}\left[B(\mu_1L_t)B(\mu_2L_t)\right]^{1/2}e^{-\pi/2\mu L_t}, \tag{3.12}$$

thus, eq. (3.11) can be written as

$$\left[\left(i\frac{d}{d\varphi_1}-\delta\alpha\right)^2-\kappa\cos\left(\varphi_1-\frac{\theta}{2}\right)\right]g(\varphi_1)=\epsilon g(\varphi_1). \tag{3.13}$$

Finally, we apply a change of variable $\varphi=\varphi_1-\frac{\theta}{2}$ and define $f(\varphi)=g(\varphi+\frac{\theta}{2})$. Then, eq. (3.13) takes the form

$$\left[\left(i\frac{d}{d\varphi}-\delta\alpha\right)^2-\kappa\cos\varphi\right]f(\varphi)=\epsilon f(\varphi). \tag{3.14}$$

According to refs. [1, 4, 5], the masses μ_1, μ_2 and the chiral condensate $-\langle\overline{\psi}\psi\rangle_\theta$ can be obtained through the following equations when $m\ll\mu$

$$\begin{aligned} \mu_2^2 &= \frac{2\pi^2}{L_t^2}\kappa\int_{-\pi}^{\pi}d\varphi\cos\varphi|f_0(\varphi)|^2,\ \ \varphi\in(-\pi,\pi), \\ \mu_1^2 &= \mu^2+\mu_2^2, \\ \langle\overline{\psi}\psi\rangle_\theta &= -\frac{\mu_2^2}{4\pi m}, \end{aligned} \tag{3.15}$$

where $f_0(\varphi)$ denotes the ground state function of eq. (3.14), which obeys $f_0(\varphi+2\pi)=f_0(\varphi)$ and has to be normalized.

Now we need to find a solution to eq. (3.14) in order to calculate μ_2; however, κ already depends on μ_2. This means that eqs. (3.12), (3.14) and (3.15) must be solved in a self consistent way. Analytically this is difficult for general values, but it can be done numerically. Still, there is one limiting case that is worth analyzing, because it will provide a cross check with the numerical solutions of the next section. Let us suppose that $\delta\alpha=0$ and $\mu L_t\gg 1$. Since $\kappa\propto L_t$ then $\kappa\gg 1$. Besides, the largest contribution of $\kappa\cos\varphi$ emerges when φ is close to zero, so we can approximate $\kappa\cos\varphi\approx\kappa-\kappa\frac{\varphi^2}{2}$. Hence

$$\mu L_t\gg 1,\ \delta\alpha=0\Rightarrow -\frac{d^2f}{d\varphi^2}-\kappa\left(1-\frac{\varphi^2}{2}\right)f=\epsilon f. \tag{3.16}$$

With the ansatz $f(\varphi) = e^{-b\varphi^2}$ we obtain

$$-\frac{d^2 f}{d\varphi^2} - \kappa\left(1 - \frac{\varphi^2}{2}\right) f = \left(-2b - 4b^2\varphi^2 - \kappa + \kappa\frac{\varphi^2}{2}\right) e^{-b\varphi^2}, \tag{3.17}$$

then

$$\epsilon = -2b - 4b^2\varphi^2 - \kappa + \kappa\frac{\varphi^2}{2}. \tag{3.18}$$

Let us remember that ϵ is a constant, so it cannot depend on φ, this forces to fix $b = \sqrt{\frac{\kappa}{8}}$. As a result, the normalized solution to eq. (3.14) under the previous assumptions is

$$f(\varphi) = \frac{1}{\int_{-\pi}^{\pi} d\varphi |e^{-\sqrt{\frac{\kappa}{8}}\varphi^2}|^2} e^{-\sqrt{\frac{\kappa}{8}}\varphi^2}. \tag{3.19}$$

We will denote

$$I \equiv \frac{\int_{-\pi}^{\pi} d\varphi \cos\varphi\, e^{-2\sqrt{\frac{\kappa}{8}}\varphi^2}}{\int_{-\pi}^{\pi} d\varphi\, e^{-2\sqrt{\frac{\kappa}{8}}\varphi^2}}, \tag{3.20}$$

in that manner we can rewrite the first line of eqs. (3.15) as

$$\mu_2^2 = \frac{2\pi^2}{L_t^2}\kappa I = \frac{8}{L_t^2\pi} m L_t \cos\frac{\theta}{2} \left[B(\mu_2 L_t) B(\mu_1 L_t)\right]^{1/2} e^{-\pi/2\mu L_t} I. \tag{3.21}$$

When $\mu L_t \gg 1$, we are able to obtain a simpler form of the $B(z)$ function in eq. (3.5). It can be seen directly from its expression, that if $z \gg 1$ the exponential term in the denominator of the integrand vanishes. Thus the integral is suppressed, together with the factor π/z. Then

$$B(z) \approx \frac{z e^{\gamma}}{4\pi}, \qquad z \gg 1. \tag{3.22}$$

With this result the value for μ_2 is approximately

$$\mu_2^2 \approx \frac{8\pi^2}{L_t^2\pi} m L_t \cos\frac{\theta}{2} \left(\frac{\mu_1 L_t e^{\gamma}}{4\pi}\right)^{1/2} \left(\frac{\mu_2 L_t e^{\gamma}}{4\pi}\right)^{1/2} e^{-\pi/2\mu L_t} I = 2m\cos\frac{\theta}{2} e^{\gamma} \mu_1^{1/2} \mu_2^{1/2} e^{-\pi/2\mu L_t} I. \tag{3.23}$$

Equation (3.15) is valid when $m \ll \mu$. That way, we can approximate μ_1 by $\mu = \sqrt{2}g/\sqrt{\pi}$, since it is its value when the fermions are massless. By taking the limit $L_t \to \infty$, it follows that $e^{-\pi/2\mu L_t} \to 1$. Now, let us analyze the integral I in eq. (3.20) by expanding $\cos\varphi$ in Taylor series

$$I = 1 + \sum_{n=1}^{\infty} \frac{\int_{-\pi}^{\pi} d\varphi \frac{(-1)^n \varphi^{2n}}{(2n)!} e^{-2\sqrt{\frac{\kappa}{8}}\varphi^2}}{\int_{-\pi}^{\pi} d\varphi\, e^{-2\sqrt{\frac{\kappa}{8}}\varphi^2}}. \tag{3.24}$$

If we take the limit $L_t \to \infty$ then $\kappa \to \infty$ and we have the following relations for the integrands of the second term in the latter expression

$$\begin{aligned} \lim_{\kappa\to\infty} \varphi^{2n} e^{-2\sqrt{\frac{\kappa}{8}}\varphi^2} &= 0, \\ \lim_{\kappa\to\infty} e^{-2\sqrt{\frac{\kappa}{8}}\varphi^2} &= A\delta(\varphi), \end{aligned} \tag{3.25}$$

where A is an irrelevant constant and $\delta(\varphi)$ is the Dirac delta. Therefore, the second term in right hand side of eq. (3.24) vanishes when $L_t \to \infty$ and we are left with $I = 1$. This can also be seen numerically, as it is shown in figure 3.1. Then, eq. (3.23) is simplified to

$$\mu_2^2 = 2e^{\gamma} m \cos\frac{\theta}{2} \mu^{1/2} \mu_2^{1/2}, \qquad L_t \to \infty,\ m \ll \mu. \tag{3.26}$$

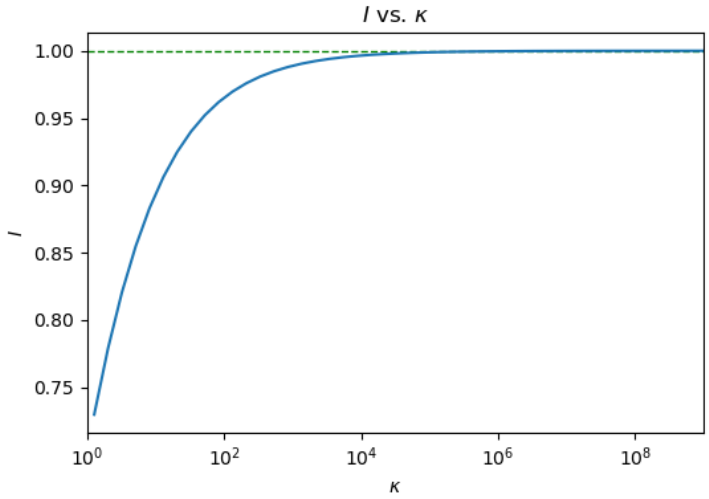

Figure 3.1: $I(\kappa)$ defined in eq. (3.24)

We are finally left with

$$\begin{aligned} \mu_2 &= \left(4e^{2\gamma}\mu m^2 \cos\frac{\theta}{2}\right)^{1/3} \\ &= \left(4e^{2\gamma}\sqrt{\frac{2}{\pi}}gm^2 \cos\frac{\theta}{2}\right)^{1/3}. \end{aligned} \tag{3.27}$$

The constant terms can be evaluated, giving

$$\left(4e^{2\gamma}\sqrt{\frac{2}{\pi}}\right)^{1/3} = 2.1633... \tag{3.28}$$

Therefore

$$\mu_2 = 2.1633... \cos\frac{\theta}{2}(m^2 g)^{1/3}, \qquad L_t \to \infty,\ m \ll \mu. \tag{3.29}$$

In the two flavor massive Schwinger model we can make the analogy of the degenerate fermions with a degenerate version of the quarks u and d. That way one can relate μ_1 with the mass of the η boson and μ_2 with the pion mass from QCD. So from now on we will denote $\mu_1 = m_\eta$ and $\mu_2 = m_\pi$. There are two predictions for m_π at infinite volume and small fermion mass m. The first one is a semi-classical prediction [6], that is equal to eq. (3.29) by taking $\theta = 0$. The other prediction was deduced by A. Smilga [7] and it is slightly different from the semi-classical one: $m_\pi = 2.008(m^2 g)^{1/3}$.

It is possible to derive more expressions for limiting cases, however, the rest of the analysis will be done numerically.

3.2 Numerical solution

The first step to solve eqs. (3.12), (3.14) and (3.15) is to find a solution of the differential equation that involves $f(\varphi)$ with the condition $f(\varphi + 2\pi) = f(\varphi)$, $\varphi \in (-\pi, \pi)$. Turns out that if one sets $\delta\alpha = 0$, performs the change of variable $\varphi = 2x$ and defines $a \equiv 4\epsilon$, $q \equiv -2\kappa$, then eq. (3.14) is taken to

$$\frac{d^2 f}{dx^2} + (a - 2q\cos 2x)f = 0, \quad f(x+\pi) = f(\pi),\ x \in \left(-\frac{\pi}{2}, \frac{\pi}{2}\right), \tag{3.30}$$

which is the quantum pendulum equation or the *Mathieu equation*, whose solutions are known as *Mathieu functions*

$$\frac{1}{\sqrt{\pi}}ce_n\left(\frac{\varphi}{2},-2\kappa\right),\ \ \frac{1}{\sqrt{\pi}}se_n\left(\frac{\varphi}{2},-2\kappa\right),\ \ n \text{ an even number due to the } 2\pi \text{ period of } f(\varphi). \tag{3.31}$$

Furthermore, if $\delta\alpha \neq 0$ one can perform the change of variable $f(\varphi) = e^{-i\delta\alpha\varphi}g(\varphi)$. Thus, the derivatives and the boundary condition become

$$\begin{aligned}\frac{df}{d\varphi} &= e^{-i\delta\alpha}\left(\frac{dg}{d\varphi} - i\delta\alpha g\right),\\ \frac{d^2f}{d\varphi^2} &= e^{-i\delta\alpha\varphi}\left(-2i\delta\alpha\frac{dg}{d\varphi} - \delta\alpha^2 + \frac{d^2g}{d\varphi^2}\right),\\ g(\varphi+2\pi) &= e^{i2\pi\delta\alpha}g(\varphi).\end{aligned} \tag{3.32}$$

Substituting in eq. (3.14) yields

$$-\frac{d^2g}{d\varphi^2} - \kappa\cos\varphi\, g = \epsilon g. \tag{3.33}$$

This is the same equation for $f(\varphi)$ when $\delta\alpha = 0$ but with a different boundary condition given by eq. (3.32)[1]. Its solutions are non periodic solutions to the Mathieu equation, better known as *Floquet solutions*. There are some analytic expressions for the Floquet solutions and for the Mathieu functions ce_n, se_n, however, they are very complex (see for example [9, 10]). The best way to proceed is by discretizing eq. (3.14) in order to get a matrix eigenvalue problem that will allows us to find the ground state function $f_0(\varphi)$.

Let us expand eq. (3.14)

$$-\frac{d^2f}{d\varphi^2} - 2i\delta\alpha\frac{df}{d\varphi} + \delta\alpha^2 f - \kappa\cos\varphi = \epsilon f \tag{3.34}$$

and divide the interval $(-\pi,\pi)$ in $N+1$ sites separated by $\Delta\varphi = 2\pi/N$. Then we interchange the continuum derivatives by discrete derivatives of second order

$$f_j = f(\varphi_j),\ \ \frac{df}{d\varphi}\to\frac{f_{j+1}-f_{j-1}}{2\Delta\varphi},\ \ \frac{d^2f}{d\varphi^2}\to\frac{f_{j+1}-2f_j+f_{j-1}}{\Delta\varphi^2},\ \ \varphi\in(-\pi,\pi),\ \ f_0 = f_N. \tag{3.35}$$

Substituting them in eq. (3.34) yields

$$-\frac{f_{j+1}-2f_j+f_{j-1}}{\Delta\varphi^2} - 2i\delta\alpha\frac{f_{j+1}-f_{j-1}}{2\Delta\varphi} + \delta\alpha^2 f_j - \kappa\cos\varphi_j\, f_j = \epsilon f_j. \tag{3.36}$$

The index j runs from 0 to $N-1$ (we are assuming $f_{-1} = f_{N-1}$ since f obeys periodic boundary). Thus we have N algebraic equations that can be written as matrices if we interchange the following

$$\frac{f_{j+1}-2f_j+f_{j-1}}{\Delta\varphi^2}\to\frac{1}{\Delta\varphi^2}\underbrace{\begin{pmatrix}-2 & 1 & 0 & 0 & \cdots & \cdots & \cdots & 1\\ 1 & -2 & 1 & 0 & \cdots & \cdots & \cdots & 0\\ 0 & 1 & -2 & 1 & \cdots & \cdots & \cdots & 0\\ \vdots & \vdots & \vdots & \vdots & \cdots & 1 & -2 & 1\\ 1 & 0 & 0 & 0 & \cdots & 0 & 1 & -2\end{pmatrix}}_{\mathbb{A}}\underbrace{\begin{pmatrix}f_0\\ f_1\\ f_2\\ \vdots\\ f_{N-1}\end{pmatrix}}_{\vec{f}},$$

[1]For this reason, eq. (3.14) is also known as the *Damped Mathieu Equation* (see e.g. ref.[8]).

$$\frac{f_{j+1}-f_{j-1}}{2\Delta\varphi} \to \frac{1}{2\Delta\varphi} \underbrace{\begin{pmatrix} 0 & 1 & 0 & 0 & 0 & \cdots & 0 & -1 \\ -1 & 0 & 1 & 0 & 0 & \cdots & 0 & 0 \\ 0 & -1 & 0 & 1 & 0 & \cdots & 0 & 0 \\ 0 & 0 & -1 & 0 & 1 & \cdots & 0 & 0 \\ \vdots & \vdots & \vdots & \vdots & \vdots & \vdots & \vdots & \vdots \\ 0 & 0 & 0 & 0 & 0 & \cdots & 0 & 1 \\ 1 & 0 & 0 & 0 & 0 & \cdots & -1 & 0 \end{pmatrix}}_{\mathbb{B}} \begin{pmatrix} f_0 \\ f_1 \\ f_2 \\ \vdots \\ f_{N-1} \end{pmatrix},$$

$$\delta\alpha^2 f_j - \kappa\cos\varphi_i f_j \to \underbrace{\mathrm{diag}(\delta\alpha^2-\kappa\cos\varphi_0, \delta\alpha^2-\kappa\cos\varphi_1, ..., \delta\alpha^2-\kappa\cos\varphi_{N-1})}_{\mathbb{C}} \vec{f}. \quad (3.37)$$

In that manner, the N algebraic equations can be expressed as

$$\left(-\frac{\mathbb{A}}{\Delta\varphi^2} - \frac{i\delta\alpha}{\Delta\varphi}\mathbb{B} + \mathbb{C}\right)\vec{f} = \epsilon\vec{f}, \quad (3.38)$$

where $\mathbb{A}$, $\mathbb{B}$, $\mathbb{C}$ and $\vec{f}$ are defined in eq. (3.37). This is a linear algebra eigenvalue problem that can be solved using subroutines of different languages (e.g. Python). Then, the eigenvectors $\vec{f}$ can be obtained, however they will not be normalized as $\int_{-\pi}^{\pi} d\varphi |f(\varphi)|^2 = 1$, so one must use a numerical integral (see Appendix B) to normalize the resultant vector $\vec{f}$. Reference [1] mentions some limiting case solutions of the ground state of eq. (3.34)

$$f(\varphi) \approx \begin{cases} \frac{1}{\sqrt{2\pi}}\left[1 + \frac{\kappa}{1-4\delta\alpha^2}(\cos\varphi - 2i\delta\alpha\,\mathrm{sen}\,\varphi)\right], & \text{for } \frac{\kappa}{1\pm 2\delta\alpha} \ll 1 \\ \frac{1}{\sqrt{2\pi}}\left[\frac{1}{\sqrt{2}}\left(1+e^{\mp i\varphi}\right) + \frac{\kappa}{4\sqrt{2}}\left(e^{\pm i\varphi}+e^{\mp 2i\varphi}\right)\right], & \text{for } \delta\alpha = \pm\frac{1}{2}, \kappa \ll 1 \\ \frac{1}{\int_{-\pi}^{\pi}|e^{-i\delta\alpha\varphi-\sqrt{\frac{\kappa}{8}}\varphi^2}|^2 d\varphi} e^{-i\delta\alpha\varphi-\sqrt{\frac{\kappa}{8}}\varphi^2}, & \text{for } \kappa \gg 1 \end{cases} \quad (3.39)$$

One can compare the numerical result with these particular expressions in order to verify the outcome of diagonalizing eq. (3.38). In figure 3.2 the comparison is shown.

The next step is to find solutions for m_π and the chiral condensate $\langle\overline{\psi}\psi\rangle = -m_\pi^2/4\pi m$. We had the following system of equations

$$\left[\left(i\frac{d}{d\varphi} - \delta\alpha\right)^2 - \kappa\cos\varphi\right] f(\varphi) = \epsilon f(\varphi),$$

$$(m_\pi L_t)^2 = 2\pi^2\kappa\int_{-\pi}^{\pi} d\varphi\cos\varphi|f_0(\varphi)|^2,$$

$$\kappa = \frac{4}{\pi}mL_t\cos\frac{\theta}{2}\left[B(m_\eta L_t)\right]^{1/2}\left[B(m_\pi L_t)\right]^{1/2} e^{-\pi/2\mu L_t}. \quad (3.40)$$

We introduce the notation $\beta = 1/g^2$.

Equations (3.40) can be solved as a non linear system of equations or in a self consistent way. Both procedures can be explained as recipes. To solve eqs. (3.40) as a non linear system one does the following steps:

- First, one has to give a value for κ, $\delta\alpha$, θ, β and m, that way m_π and L_t are not determined yet.
- Then, the ground state function is calculated numerically by using eq. (3.38) for the κ and $\delta\alpha$ we chose. The result is normalized.

- With f_0 already calculated, one computes $m_\pi L_t$ with the second equation of (3.40), using once again a numerical integrator.
- Note that $m_\pi L_t$ is already known from the last step, nevertheless, in order to find L_t and m_π one has to determine the "L_t-roots" of the last equation in (3.40). This can be done using a root finder, for instance bisection.

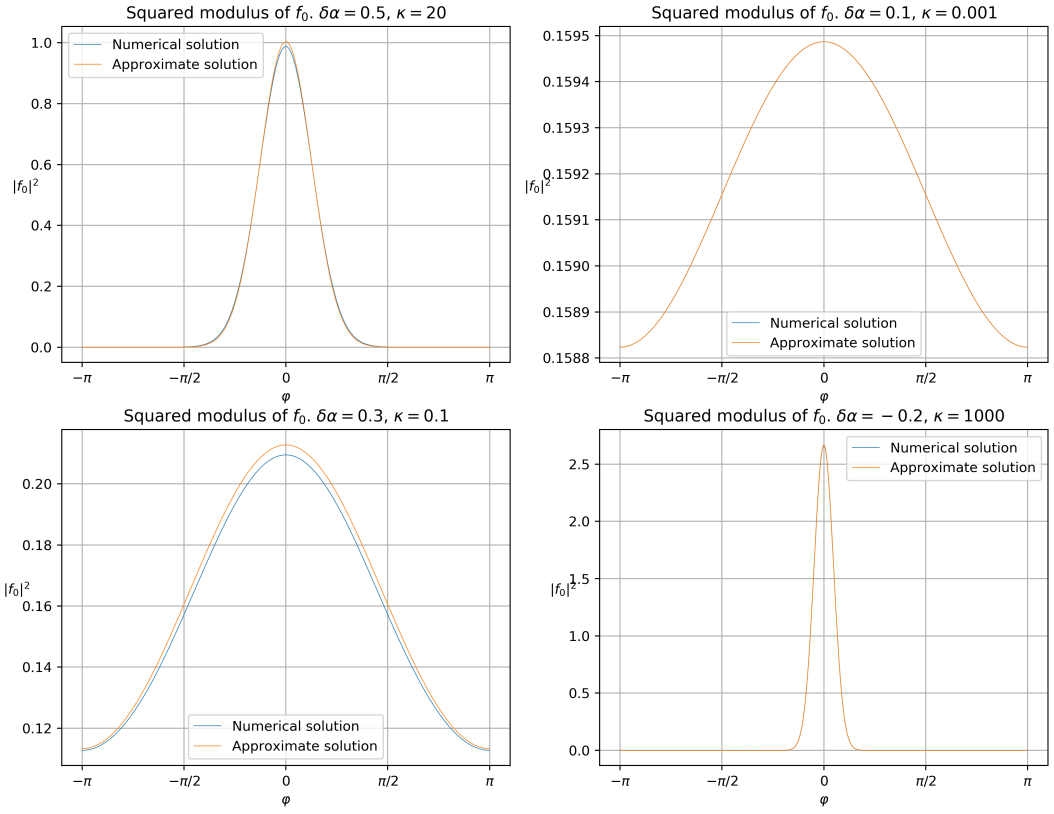

Figure 3.2: Ground sate function of eq. (3.34). The approximate solutions correspond to the expressions in (3.39). In the two right-hand side plots is hard to distinguish between both curves. $N + 1 = 1,000$ points in the discretization were used.

Following these four steps the system can be solved. It is important to note, however, that with this procedure one does not have control over L_t, but over κ, so if a solution for a specific L_t is desired, then a scan for several values of κ has to be applied. Still, it is possible to have control over L_t, but then one cannot give an initial value for m and it has to be determined in the same way we computed L_t in the last four steps. That is, one would have to do the following steps instead:

- Give a value for κ, $\delta\alpha$, θ, β, L_t and leave m_π and m undetermined.
- Calculate the normalized groundstate $f_0(\varphi)$.
- With f_0 already calculated, one computes m_π with the second equation of (3.40).
- Now one has to determine m in the last equation of (3.40). In this case one can solve for m analytically, there is no need for a root finder.

On the other hand, if one wants to have total control over both variables, L_t and m, then the system has to be solved self consistently. The idea is the following:

- Give a value for $\delta\alpha$, θ, β, L_t, m and give an initial guess of the pion mass m_π^{ini}. This last value is the one that will be determined self consistently.

- Calculate κ.
- Calculate a new value of the pion mass, m_π^{new}, using the second equation of (3.40).
- If $|m_\pi^{\text{new}} - m_\pi^{\text{ini}}|$ is smaller than an error that one desires, then m_π^{new} is the result for m_π. Otherwise, one has to use m_π^{new} as m_π^{ini} and repeat these four steps until the final value has converged within the error.

The three methods were implemented with Python and all of them give the same results. The last one can be a more expensive computationally since one does not know how long is going to take the algorithm to converge and it would depend on the initial guess. Hence, if one is not expecting results for particular values of m or L_t and instead for a wide range of them, finding solutions as a non linear system of equations can be more useful.

The first result to be revised is eq. (3.29), because it helps to verify the numerical solution and also allows to check the results with the three different methods explained above. To do so, one substitutes m_η for its value in the chiral limit ($m_\eta = \mu$) and then solves eqs. (3.40). In figure 3.3 the pion mass is shown as a function of $(m^2 g)^{1/3}$ for different values of L_t. We can see that when L_t becomes larger, the values get closer to the semiclassical prediction.

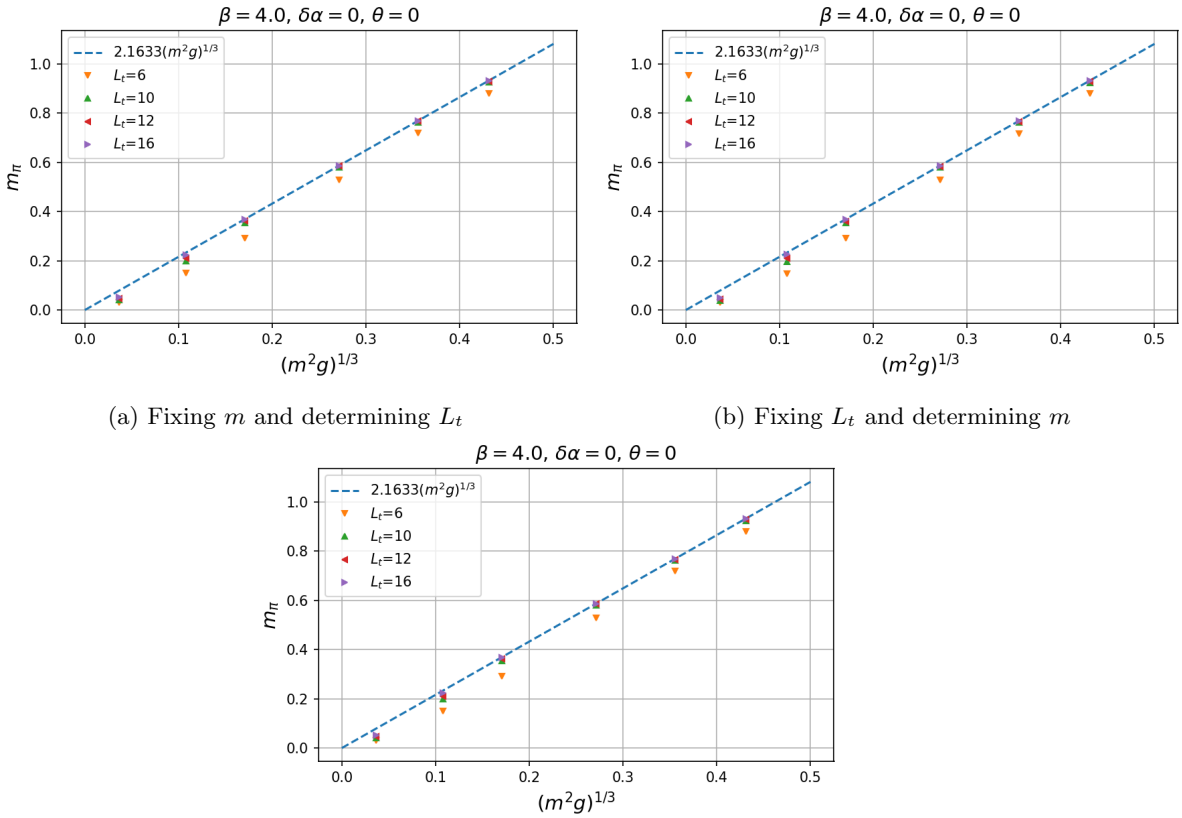

(a) Fixing m and determining L_t

(b) Fixing L_t and determining m

(c) Self consistent solution

Figure 3.3: Predictions of the pion mass as function of $(m^2 g)^{1/3}$ when one substitutes $\mu_1 \approx \mu$. Each plot was made with each one of the different methods described above. It can be seen that the result is the same.

If one does not substitute $m_\eta \approx \mu$ and instead writes $m_\eta = \sqrt{m_\pi^2 + \mu^2}$, the result of figure 3.3 is different, since m_π will not converge to eq. (3.29). In figure 3.4, the pion mass as a function of $(m^2 g)^{1/3}$ and m_η as a function of m are shown, but taking into account

the change in m_η.

The chiral condensate can be calculated as well by using the third line of eqs. (3.15). Different values of this quantity as function of L_t and the temperature are shown in figure 3.5.

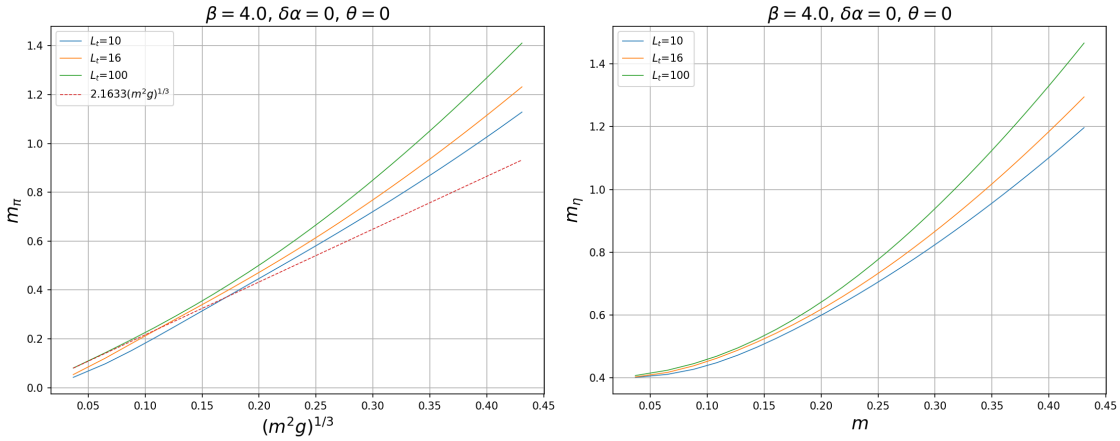

Figure 3.4: Predictions of m_η and m_π for different fermion masses and values of L_t. It can be seen that as L_t becomes larger, for small m the result gets closer to the semiclassical prediction.

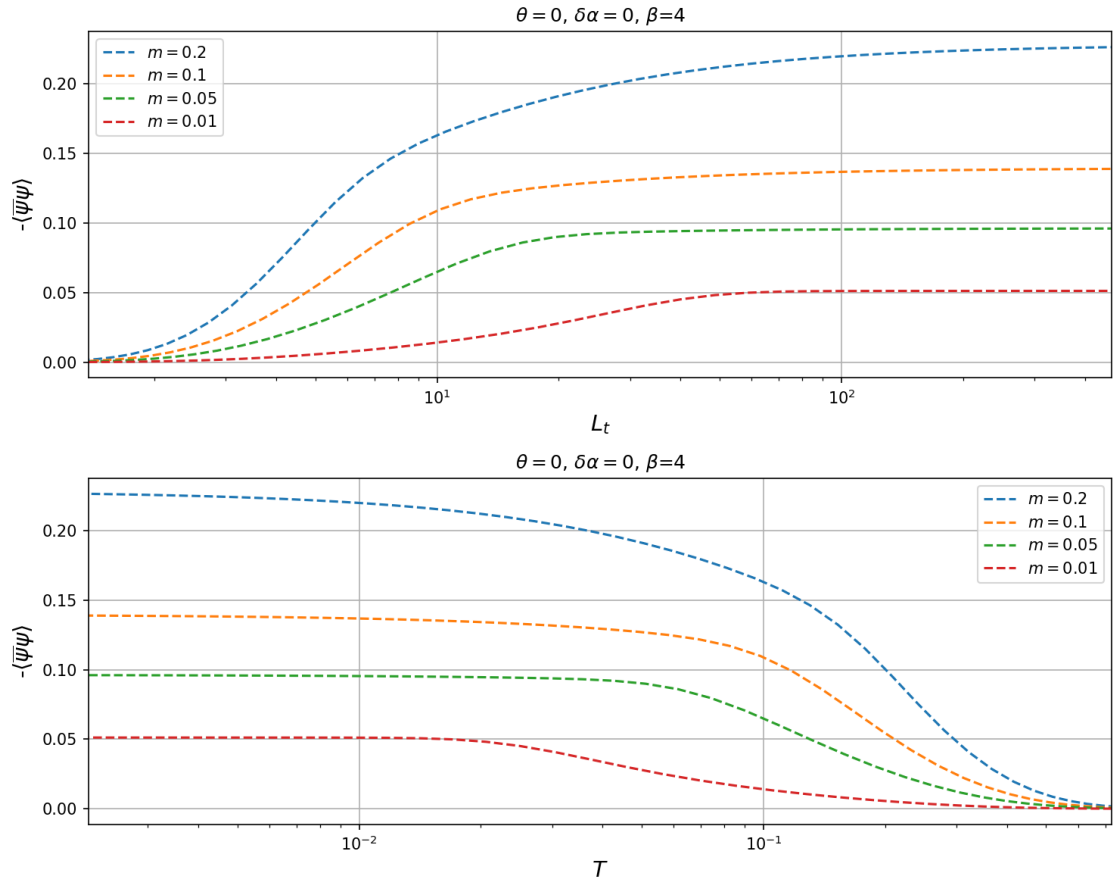

Figure 3.5: Predictions of the chiral condensate -$\langle\overline{\psi}\psi\rangle$ as a function of L_t and the temperature T. When $m \to 0$, $\langle\overline{\psi}\psi\rangle$ vanishes.

3.3 Lattice simulations results

In this section we show results of m_π and m_η obtained with lattice simulations at finite non-zero temperature for $\beta = 1/g^2 = 4$. Each value of m_π and m_η was obtained through 1,000 measurements separated by 10 sweeps. 500 sweeps were performed to thermalize the configurations. We compare the results of the simulations with the prediction given by Hosotani, by setting $\delta\alpha = \theta = 0$. In figures 3.7, 3.8 and 3.9 results of m_π vs. $(m^2 g)^{1/3}$ and m_η vs. m for a spatial volume $L = 64$ and a time extension $L_t = 10, 12, 16$ are shown, respectively. These plots are in lattice unites, *i.e.* we have set the lattice constant $a = 1$, so the masses do not have dimensions. For $\beta = 4$, the mass of η in the chiral limit is $\sqrt{2(0.5)^2/\pi} \approx 0.39$; then, one would expect Hosotani's prediction to match the simulation results when the fermion mass $m \ll 0.39$. This implies that the results should be valid when $(m^2 g)^{1/3} \ll 0.42$. From figure 3.7 we see that when $(m^2 g)^{1/3} \lesssim 0.1$ the prediction matches the results obtained with the simulations. The only difference in that region is that m_π of the simulation does not vanish in the chiral limit, this is a *finite volume effect*. For larger m both values disagree. In fact, we can see that the lattice simulations converge to the prediction by A. Smilga. Now, if $(m^2 g)^{1/3} \lesssim 0.1$, then $m \lesssim 0.044$. According to figure 3.7 (b), in this region the prediction coincides with the results from the simulation. We see that both of them converge to a value very close to 0.4, which is compatible with $m_\eta = \sqrt{2g^2/\pi}$. However, for masses larger than 0.05 there is again a discrepancy between the simulations and the analytic prediction of m_η. In figures 3.8 and 3.9 the relation between both results is the same, but for $L_t = 16$ the value measured for m_π gets closer to zero in the chiral limit. With the simulations one can obtain the chiral condensate as well. Nevertheless, one cannot compare directly this result with the prediction by Hosotani, because, as we mentioned in Chapter 2, Wilson fermions break the chiral symmetry even when $m = 0$. Therefore, we do not see that $\langle\overline{\psi}\psi\rangle$ vanishes. For instance, in figure 3.6 we show $\langle\overline{\psi}\psi\rangle$ for $L_t = 10$ and $L = 64$ as a function of the fermion mass.

Based on the results, we can affirm that the predictions of eqs. (3.40) do not allow us to make a study for masses $m \sim \sqrt{2g^2/\pi}$. However, it is still useful to compare values near the chiral limit. The approach analyzed in this chapter for the Schwinger model at finite temperature would be more useful to compare results for the boson masses and the chiral condensate for arbitrary values of θ close to $m = 0$. In principle, this is what Hosotani intended when he developed his solution. However, it is still worth to revise how far one can go with the outcome of eqs. (3.40) to study the finite temperature Schwinger model for arbitrary fermion mass.

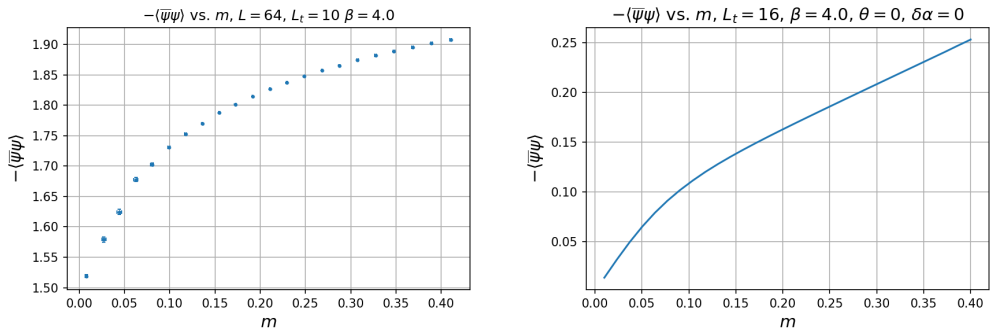

(a) $-\langle\overline{\psi}\psi\rangle$ vs. m obtained with lattice simulations.

(b) $-\langle\overline{\psi}\psi\rangle$ vs. m obtained with eqs. (3.40) and the last line of eqs. (3.15).

Figure 3.6: In the left hand plot, we show the result of $\langle\overline{\psi}\psi\rangle$ obtained with the lattice simulations, while in the right hand side we show the prediction by Hosotani. The former does not vanish in the chiral limit due to the Wilson fermions.

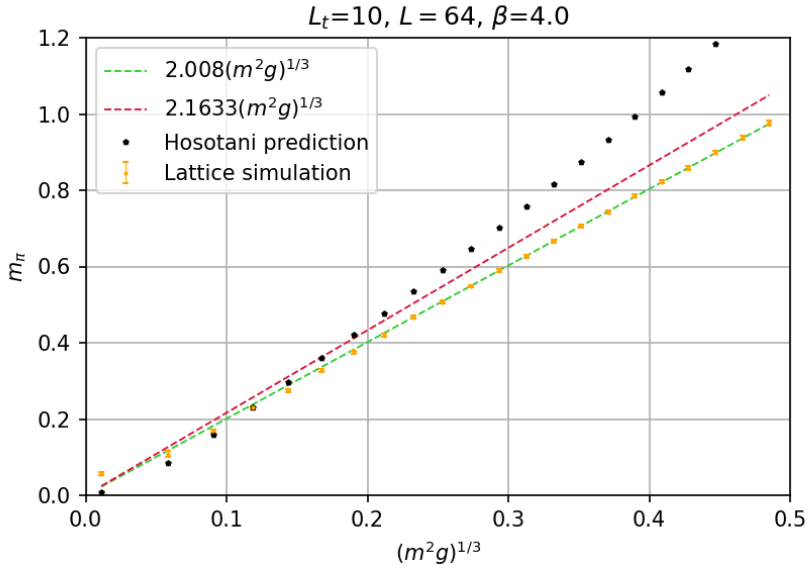

(a) m_π vs. $(m^2g)^{1/3}$

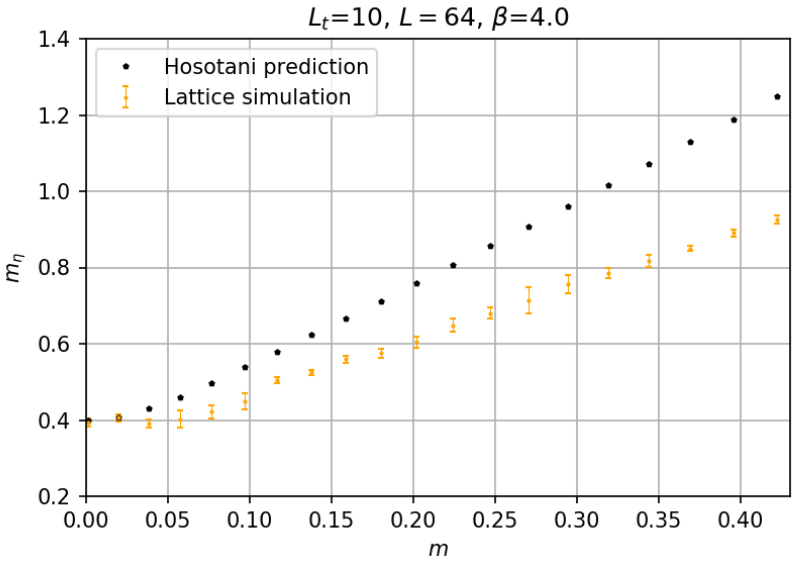

(b) m_η vs. m

Figure 3.7: Masses of the η and π mesons as a function of the degenerate fermion mass m for $L_t = 10$.

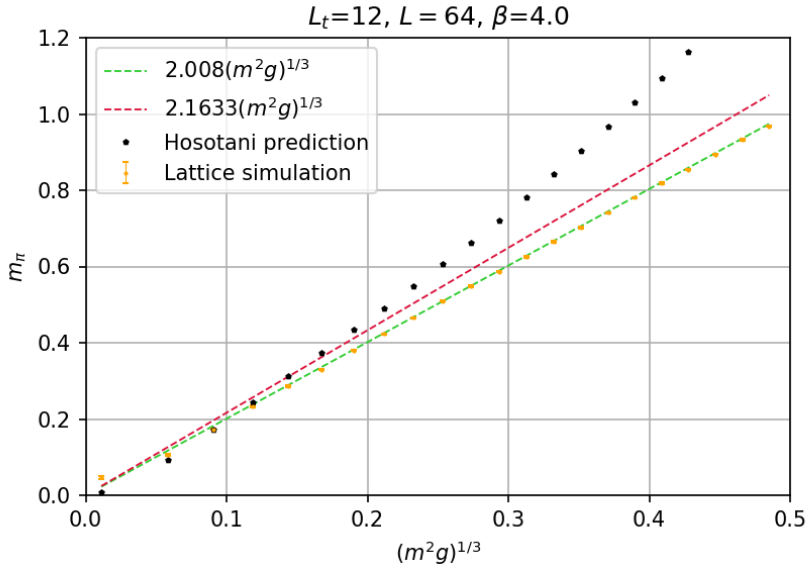

(a) m_π vs. $(m^2g)^{1/3}$

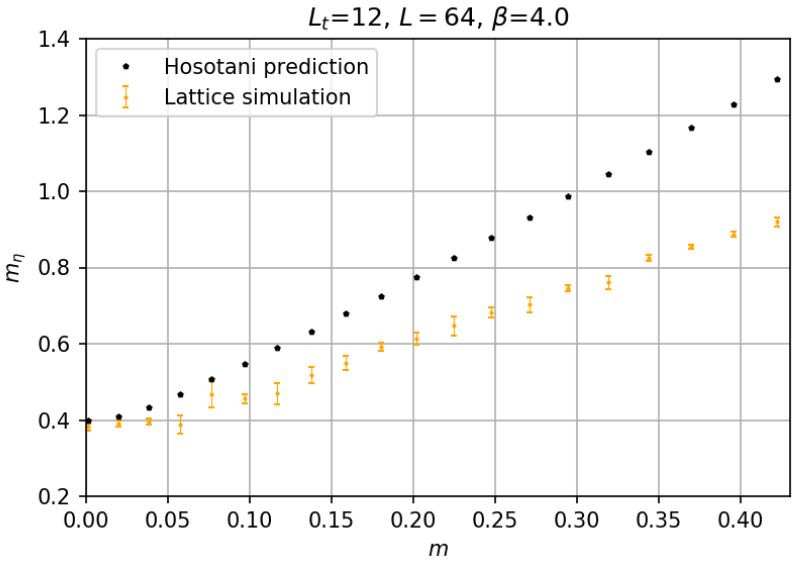

(b) m_η vs. m

Figure 3.8: Masses of the η and π mesons as a function of the degenerate fermion mass m for $L_t = 12$.

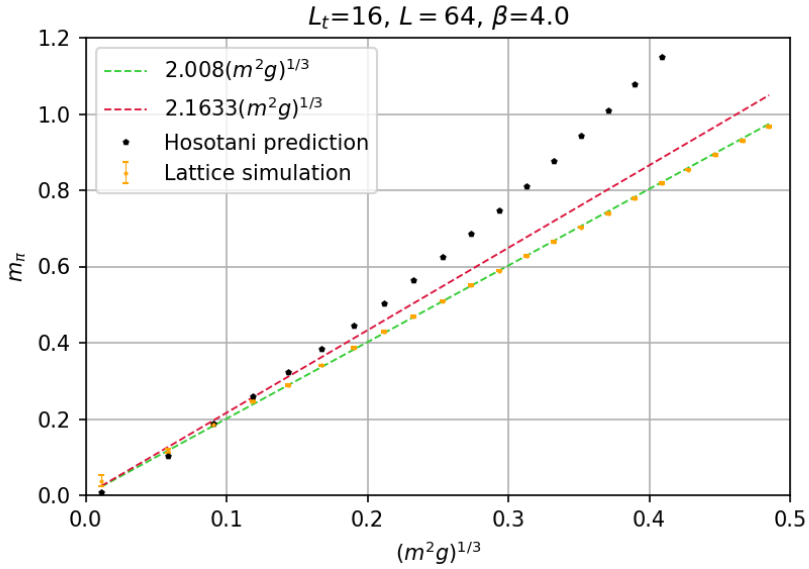

(a) m_π vs. $(m^2g)^{1/3}$

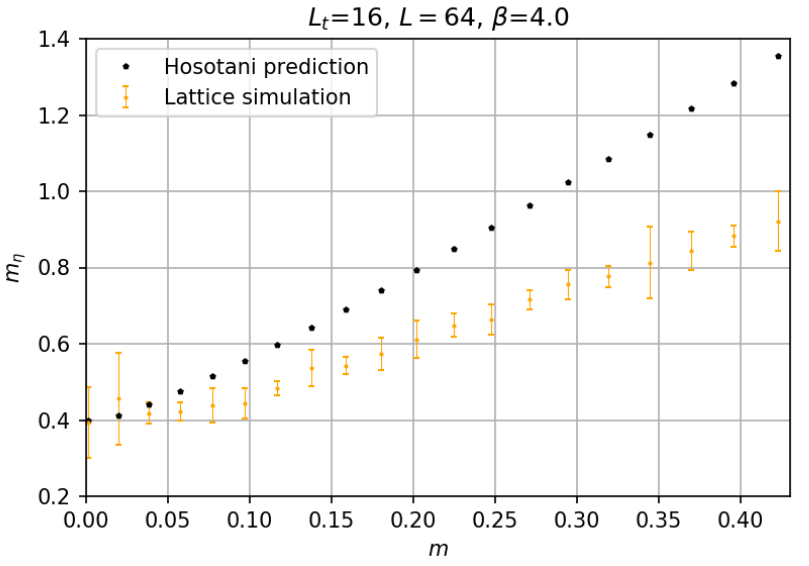

(b) m_η vs. m

Figure 3.9: Masses of the η and π mesons as a function of the degenerate fermion mass m for $L_t = 16$.

Bibliography

[1] Y. Hosotani. More about the massive multiflavor Schwinger model. In *Nihon University Workshop on Fundamental Problems in Particle Physics*, pages 64–69, 5 1995.

[2] Y. Hosotani and R. Rodriguez. Bosonized massive N-flavour Schwinger model. *Journal of Physics A: Mathematical and General*, 31(49):9925–9955, Dec 1998.

[3] Y. Hosotani and R. Rodríguez. Anomalous behavior in the massive Schwinger model. *Physics Letters B*, 389(1):121–128, Dec 1996.

[4] J. E. Hetrick, Y. Hosotani, and S. Iso. The Interplay between mass, volume, vacuum angle and chiral condensate in N flavor QED in two-dimensions. *Phys. Rev. D*, 53:7255–7259, 1996.

[5] J.E. Hetrick, Y. Hosotani, and S. Iso. The massive multi-flavor schwinger model. *Physics Letters B*, 350(1):92–102, May 1995.

[6] C. Gattringer, I. Hip, and C.B. Lang. The chiral limit of the two-flavor lattice Schwinger model with Wilson fermions. *Physics Letters B*, 466(2):287–292, 1999.

[7] A. V. Smilga. Critical amplitudes in two-dimensional theories. *Phys. Rev. D*, 55:R443–R447, Jan 1997.

[8] D. Y. Hsieh. On Mathieu equation with damping. *Journal of Mathematical Physics*, 21(4):722–725, 1980.

[9] M. Abramowitz and I. A. Stegun. *Handbook of Mathematical Functions with Formulas, Graphs, and Mathematical Tables*. Dover, New York, ninth dover printing, tenth gpo printing edition, 1964.

[10] N. W. McLachlan. *Theory and application of Mathieu functions*. Clarendon Press, Oxford, 1951.